Applied Catalysis B: Environmental 338 (2023) 123066

Contents lists available at ScienceDirect

Applied Catalysis B: Environmental

journal homepage: www.elsevier.com/locate/apcatb

Hierarchical zeolites TNU-9 and IM-5 as the catalysts for cracking processes

Karolina A. Tarach [a,*], Joaquin Martinez-Triguero [b], Susana Valencia [b], Kamila Wojciechowska [a], Fernando Rey [b], Kinga Góra-Marek [a,*]

[a] Faculty of Chemistry, Jagiellonian University in Kraków, Gronostajowa 2, 30-387 Kraków, Poland
[b] Instituto de Tecnología Química, Universidad Politécnica de Valencia, Camino de Vera s.n., 46022 Valencia, Spain

ARTICLE INFO

Keywords:
Hierarchical zeolites
TNU-9 and IM-5 catalysts
Fluid catalytic cracking
Low-density polyethylene
Polypropylene

ABSTRACT

The 10-ring zeolites TNU-9 and IM-5 were obtained by a desilication and evaluated in series of acid-catalysed cracking reactions. *n*-Decane and 1,3,5-tri-iso-propylbenzene cracking were performed as model reactions, while vacuum gas oil, polypropylene and polyethylene were cracked into add-value lower molecular weight chemicals. The catalytic performance improvement of hierarchical zeolites was rationalized by deep acid sites characterization in situ FT-IR studies of pyridine, carbon monoxide and 2,6-di-tert-butylpyridine sorption. Further, *operando* FT-IR-GC studies supported by 2D COS (two-dimensional correlation) analysis provided insight into cracking and coking of catalysts during polypropylene and polyethylene decomposition. It was found that NaOH-derived catalysts ensure the most upsurged acidity, in terms of number and accessibility of the sites, and then with better performance. In VGO cracking the connected mesopores added post-synthesis increased yields to propylene and middle distillates and lowered coke production. A bigger share of *iso*-olefins was observed both in VGO and polyolefins cracking products.

1. Introduction

Polypropylene (PP) and polyethylene (PE) are the widely applied polyolefins accounting for more than $^2/_3$ of the annual plastics production. This rapid development of the polymer industry implies the search for innovative methods for waste plastic conversion into the transportation fuels or higher value (petro)chemicals [1]. A number of approaches can be applied to convert plastic residues into chemical or fuel precursors. Depolymerisation to monomers is one of the ways to chemically recycle plastic waste. This method is generally employed for some polyamides and polyesters but not to polyolefins which thermal cracking results in the formation of a wide spectrum of hydrocarbons distribution. Further processing is therefore necessary to meet the requirements of high-value chemicals. More beneficial is catalytic cracking offering under milder operating conditions both higher activity and possibility to regulate the product distribution. Thus the catalytic cracking offers the highest valorization of plastic waste for production of fuels and value-added chemicals. According to review of Palos et al. [2] the conventional refinery units for fluid catalytic cracking are expected to be capable of recycling the plastic waste on large-scale and cofeeding polyolefins with vacuum gas oil (VGO) without affecting the yields and quality of the product streams. The commercial equilibrated FCC catalyst has proven that with low cost the catalytic pyrolysis of plastic waste might be integrated in a refinery providing light olefin and gasoline fractions [3].

The first reports about the catalytic cracking of polypropylene and polyethylene plastics focused on conventional zeolites, such as ZSM-5 [4,5] and USY [5] as catalysts. The acid sites located in well-defined micropores contribute to the appearance of the C_2–C_4 olefins, and usually, the higher the strength of the acidic sites is, the more effective the cracking of the polymer [6–9]. Further, ZSM-5 zeolite was identified as an excellent additive for FCC catalyst allowing to increase the light olefins yield [10,11]. In the case of cofeeding VGO with 10 wt% of polyethylene or polypropylene during cracking over commercial equilibrated FCC catalyst with ZSM-5 zeolite as an additive the products distribution was affected by increased yield of olefins, while aromatics, paraffins, and coke were reduced [12]. The promising results for ZSM-5 zeolite are driving force to study other 10-ring zeolites as catalysts of vacuum gas oil cracking and polymers [13]. The enhanced activity upon development of hierarchical pore system in ZSM-5 zeolite has been already proven in cracking of vacuum gas oil and polymers [14,15]. The size of microvoids in ZSM-5 zeolite at the channels intersections contribute to the type of products formed, thus selectivity of the hydrocarbon reactions. The microporous structure gives however a

* Corresponding authors.
E-mail addresses: karolina.tarach@uj.edu.pl (K.A. Tarach), kinga.gora-marek@uj.edu.pl (K. Góra-Marek).

https://doi.org/10.1016/j.apcatb.2023.123066
Received 10 March 2023; Received in revised form 30 June 2023; Accepted 30 June 2023
Available online 1 July 2023
0926-3373/© 2023 The Authors. Published by Elsevier B.V. This is an open access article under the CC BY license (http://creativecommons.org/licenses/by/4.0/).

negative impact to activity and deactivation of the catalyst due to limited molecular transport of the reagents, particularly branched molecules. The severe diffusion restrictions resulting in limited use of acidic sites can be alleviated in the presence of hierarchical zeolites where secondary mesoporosity is generated in the pristine microporous zeolite [16]. The shortening of the diffusion path improves the accessibility of the acidic sites. The hierarchical zeolites with unique zeolite acidity and improved transport of reagents constitute therefore the catalysts particularly designed for the catalytic cracking of polyolefinic plastic waste.

In the present work we investigated the applicability of 10-ring hierarchical zeolites TNU-9 and IM-5 and their purely microporous counterparts in relevant cracking reaction including vacuum gas oil, *n*-decane, and 1,3,5-tri-iso-propylbenzene as well as polypropylene and polyethylene into useful lower molecular weight molecules. The various volume of internal cavities and pore topology of TNU-9 and IM-5 zeolites is expected to provide differentiated susceptibility to desilication process and catalytic activity. We demonstrate that secondary mesoporosity improves the catalytic performance by increasing its overall gas oil and polymer cracking activity and offering better selectivity. In gas oil cracking higher yields to propylene and middle distillates as well as lower coke production while bigger share of *iso*-olefins were observed. The work is aimed to assess the catalytic potential of 10-ring IMF and TUN structures for the valorization of polymer wastes to petroleum derivatives. The fluid catalytic cracking (FCC) units possess both the capacity and versatility for polyolefinic plastics (polyethylene and polypropylene) to be co-fed together with the current streams of the industrial units [17]. As far as the use of the FCC units for the production of fuels and raw materials would promote the economy of the recycling process still the significant research is needed to tailor the properties of catalysts [18].

2. Experimental

2.1. Catalyst preparation

Zeolite TNU-9 was prepared by hydrothermal synthesis in PTFE-lined stainless steel autoclaves at 160 °C under rotation using 1,4-dibromobutane (1,4-DBB) and 1-methylpyrrolidine (1-MP) as organic structure directing agents (OSDAs). The gel preparation was based on procedures reported previously [19] and consisted of mixing an aqueous solution of sodium hydroxide with silica (Aerosil 200, Degussa) followed by the addition of an aqueous solution of $Al(NO_3)_3{\cdot}9\,H_2O$. The gel is kept under stirring for 10 min, then the required amounts of 1-MP and 1, 4-DBB are subsequently added and the mixture is stirred for one hour. The chemical composition of the synthesis gel was as follows: SiO_2: 0.017 Al_2O_3: 0.37 Na_2O: 0.15 (1,4-DBB): 0.45 (1-MP): 40 H_2O.

After the required crystallization time (7–10 days), the autoclaves were cooled to room temperature and the zeolite was recovered by filtration and extensive washing with deionized water followed by drying at 100 °C. Next, the zeolite was calcined at 580 °C in static air for 3 h to remove occluded organic molecules.

Zeolite IM-5 was prepared by hydrothermal synthesis in PTFE-lined stainless steel autoclaves at 175 °C under rotation using 1,5-bis(methylpyrrolidinium)pentane dibromide (*R*) as organic structure directing agent. The OSDA was synthesized by reacting 1-methylpyrrolidine and 1,5-dibromopentane in acetone solvent under reflux conditions. The gel preparation procedure was based on reported recipes [20,21] and can be described as follows: the required amount of silica (Aerosil 200) was added to a solution of the OSDA in water under agitation. Then, an aqueous solution of sodium aluminate (54% Al_2O_3, 33% Na_2O, Carlo Erba) and sodium hydroxide were added and the mixture was stirred for 30 min. The chemical composition of the synthesis gel was as follows: SiO_2: 0.028 Al_2O_3: 0.28 Na_2O: 0.17 *R*: 40 H_2O.

After the required crystallization time (about 14 days), the autoclaves were cooled to room temperature and the zeolite was recovered by filtration and extensive washing with deionized water followed by drying at 100 °C. The synthesized solid was calcined at 580 °C in static air for 3 h to eliminate organic molecules.

Native TNU-9 or IM-5 zeolites were subjected to desilication process in 0.2 M NaOH solution. Desilication was performed in 65 °C for 30 min. The 50 ml of solution was added to 1.5 g of zeolite. After desilication the suspension was cooled down in ice-bath, filtered and washed with deionized water until neutral pH. Obtained material was ion-exchanged in 0.5 M NH_4NO_3 performed at 60 °C for 1 h. Finally, the zeolites were again filtrated, washed and dried at room temperature. The calcination of ion-exchanged samples was at 550 °C in static air for 2 h, with heating rate of 2 °C min^{-1}.

2.2. Characterization methods

Si and Al concentrations in the native zeolites TNU-9 and IM-5 as well in their NaOH-treated counterparts were determined by the ICP OES method with an Optima 2100DV (PerkinElmer) spectrometer.

The powder X-ray diffraction (XRD) measurements were performed using a PANalytical Cubix diffractometer, with CuKa radiation, λ = 1.5418 Å and a graphite monochromator in the 2Θ angle range of 2–40°. The relative crystallinity value (%Cryst) was calculated from the intensity of the XRD peaks in the range between 22.0° and 27.0°.

The N_2 sorption processes at –196 °C were carried out with an ASAP 2420 Micromeritics instrument after evacuation of the materials in vacuum at 450 °C for 12 h. Surface area (S_{BET}) and micropore volume (V_{micro}) were calculated by applying the BET and t-plot methodology, respectively. Volume of mesopores (V_{meso}) and pore size distribution were determined according to the BJH model to the adsorption branch of the isotherm. The mesopore surface area (S_{meso}) was calculated in the range between 2 and 30 nm with BJH model.

Transmission electron microscopy investigations were performed with a Philips CM-10 microscope operating at 100 kV. The samples were dispersed in 2-propanol and sonicated for 15 min before being dropped on a carbon-coated copper grid.

Prior to the FTIR study all samples were pressed into the form of self-supporting wafers (ca. 5–10 mg cm^{-2}) and pre-treated in situ in home-made quartz IR cell at 550 °C under vacuum conditions for 1 h. The IR spectra were recorded with a Bruker Invenio X spectrometer equipped with a MCT detector. The spectral resolution was 2 cm^{-1}.

The concentration of acid sites was assessed in quantitative IR studies with pyridine (Py $\geq$ 99.8%, Sigma-Aldrich), in line with the procedure given in ref. [22]. The values of 0.10 $cm^2 \mu mol^{-1}$ and 0.07 cm^2 μmol^{-1} were applied for the 1450 cm^{-1} band of pyridine coordinatively bonded to Lewis sites (PyL) and for the 1540 cm^{-1} band of pyridinium ion (PyH^+), respectively.

Quantitative approach of the sorption of pivalonitrile (Pn $\geq$ 99.8%, Sigma-Aldrich) and 2,6-di-tert-butylpyridine (dTBPy>99.8%, Sigma-Aldrich) was applied to determine the number of protonic sites exposed on the mesopore surface. The catalysts were saturated with the Pn and dTBPy vapor at room temperature, then gaseous and physisorbed phase were removed by the 10 min evacuation at room temperature and 200 °C, respectively. The maximum intensities of the bands of pivalonitrile interacting with the Si-(OH)-Al groups (at 2258–2278 cm^{-1}) and $dTBPyH^+$ ions (at 1615 cm^{-1}) together with their absorption coefficients [23,24] were taken to calculate the number of Brønsted acid sites accessible for both probes.

The acid strength was determined in pyridine thermodesorption and carbon monoxide (CO) adsorption studies. In the Py-thermodesorption experiments, the conservation of the 1450 cm^{-1} and 1540 cm^{-1} rising from Py-Lewis adducts and PyH^+ ion bands, resp., under the desorption procedure at 500 °C were taken as a measure (C_{Py}^{500} /C_{Py}^{170} where C_{Py}^{170} and C_{Py}^{500} are the intensities of IR bands of PyH^+ ions upon the evacuation at 170 °C and 500 °C, respectively) of the acid strength of the sites.

The sorption of CO (Linde Gas Poland, 99.95%) was performed at −120 °C. The downshift of the acidic hydroxyls Si(OH)Al band

(3200−3800 cm^{-1}) due to its interaction with CO molecules was taken as a measure of the acid strength.

2.3. n-Decane, 1,3,5-tri-iso-propylbenzene (TIPB) and vacuum gas oil (VGO) catalytic cracking

The cracking experiments were carried out in a MAT (Micro Activity Test) unit described previously [21,22]. For each material (fraction of the 0.59–0.84 mm), catalytic experiments were performed, preserving the amount of catalyst (cat) constant and varying feeds amounts (oil). Four cracking reactions with different cat-to-oil ratios of 1,3,5-tri-iso--propylbenzene (TIPB) were performed at 500 ºC and for 60 s time on stream (TOS), with 200 mg of catalyst. For *n*-decane cracking at 500 ºC and for 60 s TOS, 300 mg of catalyst was diluted in 2.5 g of inert silica, and five experiments were carried out. For first and last experiments the amount of feed was maintained in order to investigate the stability of catalysts. In case of gas oil cracking five experiments with different cat-to-oil ratio were also performed and 500 mg of catalyst was diluted in 2.5 g of inert silica; with reaction temperature of 520 ºC and with TOS of 30 s. Gaseous products were analysed by Gas Chromatography in a Rapid Refinery Gas Analyser from Bruker (450-GC) and simulated distillation of liquids in a Bruker SIMDIS.

Kinetic rate constants (K) were calculated by fitting the conversions (X) to a first-order kinetic equation for a plug flow reactor (1) for *n*-decane and TIPB or to a second order kinetic equation for a plug flow reactor (2) for gas oil, assuming that the deactivation is enclosed in the kinetic constant and taking into account the volumetric expansion factor (3),

$$K = -(\text{cat oil}^{-1}\text{TOS})^{-1}[\varepsilon X + (1+\varepsilon)\ln(1-X)] \quad (1)$$

$$K = -(\text{cat oil}^{-1}\text{TOS})^{-1}[X/(1-X)] \quad (2)$$

$$\varepsilon = (\Sigma\text{molar selectivities of products}) - 1 \quad (3)$$

These rate constants were used to compare the activities of the catalysts with their textural and acidic properties.

The evaluation of the catalysts studied in cracking reactions was performed with use of vacuum gas oil as the feed of the composition listed in the Table 1. Detailed description of the catalytic tests is presented in Table 2.

Table 1
Reference VGO feedstock composition.

Properties	Values
density (15 °C)	0.9172 g/cm^3
aniline point (°C)	79.2
sulfur (%)	1.65
Metal content	
N_2 (ppm)	1261
Na (ppm)	0.18
Cu (ppm)	< 0.1
Fe (ppm)	0.30
Ni (ppb)	0.2
V (ppb)	0.40
Group composition	
Average molecular weight	407
aromat. carb. (ndM%)	22.96
naphten carb. (ndM%)	15.16
paraff. carb. (ndM%)	61.88
arom. rings./molec. (ndM)	1.17
napht. rings./molec. (ndM)	1.01
ASTM D1160 (∘C)	
5%	319
10%	352
30%	414
50%	436
70%	459
90%	512

2.4. Thermogravimetric analysis of polypropylene and polyethylene catalytic cracking

For the catalytic tests polypropylene (PP, Sigma-Aldrich, product No.: 428116, Lot No.: MKCH4322, M_w of 12,000, M_n of 5000 density of 0.9 g/ml, average size 0.4 mm) and low-density polyethylene (LDPE, Alfa Aesar, product no.: 42607, lot no.: P28D047) were crushed, powdered and sieved (250 μm). The catalytic cracking was assessed by thermogravimetric analysis using a TGA/SDTA Mettler Toledo apparatus. The zeolite powder (10 mg) together with polymer (30 mg) were mixed (10 min) in an agate mortar then a ca. 10 mg of the prepared mixture was pressed (2 atm) in the form of disc (0.2 cm^2), then transferred to α-Al_2O_3 crucible and weighted with Mettler Toledo balance before the analysis. Decomposition of polymers was carried out in a temperature range from 30 ºC to 600 ºC at the heating rate of 5 ºC min^{-1} under N_2 flow (80 ml min^{-1}). In the conversion calculations, the catalyst weight and adsorbed moisture content were considered. For comparative purposes polymers were cracked without the aluminosilicate catalysts addition. The coke content was calculated from TGA experiments. After the polymer cracking, the sample in flow of N_2 was cooled down to room temperature and then was subjected to coke burning off with a rate 30 ºC min^{-1} to 800 ºC in flow of synthetic air (80 ml min^{-1}) till no mass change was observed.

2.5. FT-IR operando catalytic studies of PP and LDPE cracking

The *operando* system connected to a flow set-up was also used to investigate the degradation of PP and LDPE. For this purpose, in a custom-made 2 cm^3-volume quartz IR cell the self-supporting disc (ca. 5.5–6 mg cm^{-2}) consist of the catalyst and PP (or LDPE) mixed in 1:1 ratio was placed. The custom-made spectroscopic cell is delivered by MeasLine (www.measline.com) company under a licensed patent (PL232633, Poland). The homogeneity of the zeolite/catalyst mixture used for TGA and *operando* purposes were followed by the comparison of their IR spectra collected at room temperature and normalized to the same intensity of the overtone bands (2050–1800 cm^{-1}). Each catalyst was reflected in the same intensity of the bands 2960 cm^{-1} (–CH_3 group) and 2925 cm^{-1} (–CH_2 group), thus the equal proportion of PP and LDPE in all materials. Under the reaction conditions, the catalyst surface as well as gas phase were simultaneously monitored. As a carrier gas nitrogen (30 ml min^{-1}) being introduced by Teflon lines (1/16″), kept at 110 °C was used. The *operando* IR cell with placed catalyst disc was rapidly heated from room temperature up to 250 ºC with ramping rate of 10 ºC/s. The PP and LPDE cracking tests were performed at 250 ºC till the polymers entire decomposition was observed. Time-resolved FT-IR spectra were collected on a FT-IR spectrometer Vertex 70 (Bruker) equipped with MCT detector of the spectral resolution of 2 cm^{-1} and the 80 kHz scanner velocity. In parallel to spectroscopic observations, the reaction products were simultaneously analysed by mass spectrometry (MeasLine, www.measline.com, RGA200) as well as gas chromatography (Agilent Technologies 7890B). In the selectivity of the catalysts, the resulting coke and tar were considered.

3. Results and disscussion

3.1. Structural and textural properties

The results of the chemical analysis evidence the decrease of Si/Al ratios in hierarchical materials with respect to the native zeolites (Table 3) approving the extraction of silicon atoms from the zeolite framework. The XRD patterns (Fig. 1) depict the typical diffraction peaks of TNU-9 and IM-5 zeolites. Slight loss of the crystallinity (Table 3) observed for NaOH-treated TNU-9 and IM-5 can be indicative for distinctive mesopore formation [25]. The N_2-isotherms measured for the native TNU-9 and IM-5 zeolites were recognized as the type I of purely microporous materials (Fig. 1) with the minor value of mesopore

Table 2
Catalytic tests conditions.

Reagent	Conditions
***n*-decane**	temperature of reaction: 500 ºC; TOS = 60 s; catalyst: 500 mg, fraction 0.59–0.84 mm + 2.5 g SiO_2, fraction 0.2–0.4 mm
TIPB	temperature of reaction: 500 ºC; TOS = 60 s; catalyst: 200 mg, fraction 0.59–0.84 mm
VGO	temperature of reaction: 520 ºC; TOS = 30 s; catalyst: 500 mg, fraction 0.59–0.84 mm + 2.5 g SiO_2, fraction 0.2–0.4 mm

Table 3
Relative crystallinity values (%), chemical composition and textural parameters for the native TNU-9 and IM-5 and zeolites treated with 0.2 M NaOH solution.

Zeolite	Rel. Cryst.[a]	Si/Al	S_{BET}	S_{meso}	S_{micro}	V_{meso}	V_{micro}
	%	-	m^2g^{-1}			cm^3g^{-1}	
TNU-9	100	14.6	362	20	342	0.03	0.17
TNU-9/NaOH	85	11.1	450	103	347	0.11	0.17
IM-5	100	11.9	315	10	305	0.02	0.15
IM-5/NaOH	90	10.0	367	80	287	0.08	0.14

[a] Relative crystallinity (in %) of hierarchical materials was designated as the ratio of the sum of the integral intensity of the most intense reflections within the 2Θ angle range from 22° to 27° to the sum of integral intensity for native zeolite.

surface area (20 and 10 m^2g^{-1}, respectively). The preserved microporosity features, i.e. micropore volumes values, for NaOH treated zeolites (0.17 and 0.14 cm^3g^{-1}, respectively) allow for excluding the amorphization as responsible for observed decrease of crystallinity. (Table 3). A higher adsorption capacity in the mesopore range of the hierarchical zeolites is evidenced by a larger uptake of N_2 at high relative pressures. Undoubtedly, the adsorption isotherms can be classified as type IV isotherms of micro-mesoporous materials. While TNU-9 is a 3-dimmensional framework with large pocket intersections, IM-5 shows more limited connectivity between bidimensional channels [26]. It has the implications in the different formation of mesoporosity by OH^- attack. Indeed, the external surface area sharply increased from 20 m^2g^{-1} of untreated TNU-9 sample to 103 m^2g^{-1} for TNU-9/NaOH while for NaOH-treated IM-5 sample the extent of mesopore surface formation is smaller.

The TEM micrographs (Fig. 1) also evidence that a worm-like mesopore system spreads through the whole zeolite TNU-9 particles. In the case of IM-5 zeolite, leaching with NaOH modifies the inner part of the particle to a smaller extent than the external zone of crystals, thus the desilication results in formation mesopores directed by 2D 10-ring channels topology. Further, this limited desilication is also reflected in the Si/Al ratio, the value changes slightly suggesting higher resistance of IMF structure against OH^- ions. The mesoporosity in IM-5 materials treated with NaOH spreads up to 10 nm, while in TNU-9/NaOH also wider mesopores are formed, this can be inferred from BJH pore size distribution analysis of the N_2 adsorption isotherms (Fig. 1). The development of mesopore surface area can be also identified in the region of the O-H stretching vibrations (Fig. 2A). The significant increase in the intensity of the band of silanols groups (3745 cm^{-1}) represents the enhanced population of isolated Si-OH groups on newly fabricated mesopore system in both TNU-9/NaOH and IM-5/NaOH. The generation of large amount of silanols; i.e. weak acid sites of the strength high enough to be active in retention of reagent molecules, is one of the major functions of desilication.

3.2. The acidic properties evaluation

Acidic function of hierarchical zeolites is dependent on the nature of acid sites altered during the fabrication of the secondary system of mesopores. Desilicating medium influences the type, distribution, strength and hydrothermal stability of acid sites. When describing the factors vital for catalytic applications of hierarchical zeolites the detailed characterization of acidic properties has to be provided.

3.2.1. Nature, concentration and strength of acid sites

Assessing the acidic function of porous materials requires the methodology allowing for discriminating Brønsted and Lewis acid sites of various nature and location. Such possibility can be realized only in quantitative FT-IR studies with employment of probe molecules of various kinetic diameter. The 10-ring channel system does not limit diffusion of pyridine (Py) thus acidic properties of the zeolites were quantitatively validated with use of Py as a probe according the procedure described elsewhere [9,22]. The interaction of Py with acid sites results in the appearance of the 1540 cm^{-1} and 1450–1440 cm^{-1} bands when Brønsted and Lewis sites, respectively, are populated on the surface of solid. The values of the acid site concentrations in the zeolites were determined with the use of the absorption coefficient previously determined [9,22] for 10-ring zeolite ZSM-5 (Table 2).

The population of Lewis sites in native TNU-9 and IM-5 zeolites do not exceed 9% of the total number of Al atoms. The Al atoms are predominantly involved into formation of the Si(OH)Al group while only fraction of existing Lewis acid sites is easily accessible for Py molecule. The increase of the Al concentration (decrease of Si/Al ratio) in the NaOH-leached materials (Table 4) is identified with the concurrent formation of Brønsted and Lewis acid sites. While a small increase in intensity of the ≈ 3615 cm^{-1} band of the Si(OH)Al groups (Fig. 2) confirms the higher density of the Brønsted sites, low-temperature sorption of carbon monoxide proves the presence of Lewis acid sites in hierarchical zeolites (CO band at 2226 cm^{-1}) (Fig. 2B). The Al species being co-extracted with Si atoms from zeolite framework can be partially integrated into the mesopore walls giving rise to Brønsted and mainly Lewis acid sites, the latter due to mesoporous-like Si(OH)Al sites susceptibility towards dehydroxylation [27]. The mesoporous-like Si(OH)Al groups in hierarchical zeolites are less resistant against the thermal treatment as can be derived from the highest intensity of the 2226 cm^{-1} band of CO interacting with Lewis sites of high strength. Consequently, the predominant fraction of Lewis acid sites in hierarchical TNU-9/NaOH and IM-5/NaOH comes from dehydroxylation, some fraction of Al atoms can be considered however as extraframework Al-species, EFAl, being manifested by low intensity CO band at 2180 cm^{-1}. The Lewis acid sites formed in dehydroxylation are situated on the mesopores walls thus they are easily available for reagent molecules. Desilication results also in the appearance of some non-acidic Al-OH groups (3666 cm^{-1}), however their population is marginal in the hierarchical zeolites evidencing again no distortion of the zeolite frameworks.

The above considerations bring up a significant problem in the hierarchization of zeolites due to the fact that changes in the acid strength of the Brønsted and Lewis sites cannot be easily predicted, as in the case of non-mesoporous zeolites. Assessing the strength of Brønsted and Lewis sites also requires the refinement between the input of Brønsted and Lewis acid sites to overall acid strength. Thus, information on the acid strength of Brønsted and Lewis acid sites was derived from the Py-thermodesorption experiments (Table 4). Additional information on the Si(OH)Al groups strength was obtained from the scrutiny of the O–H

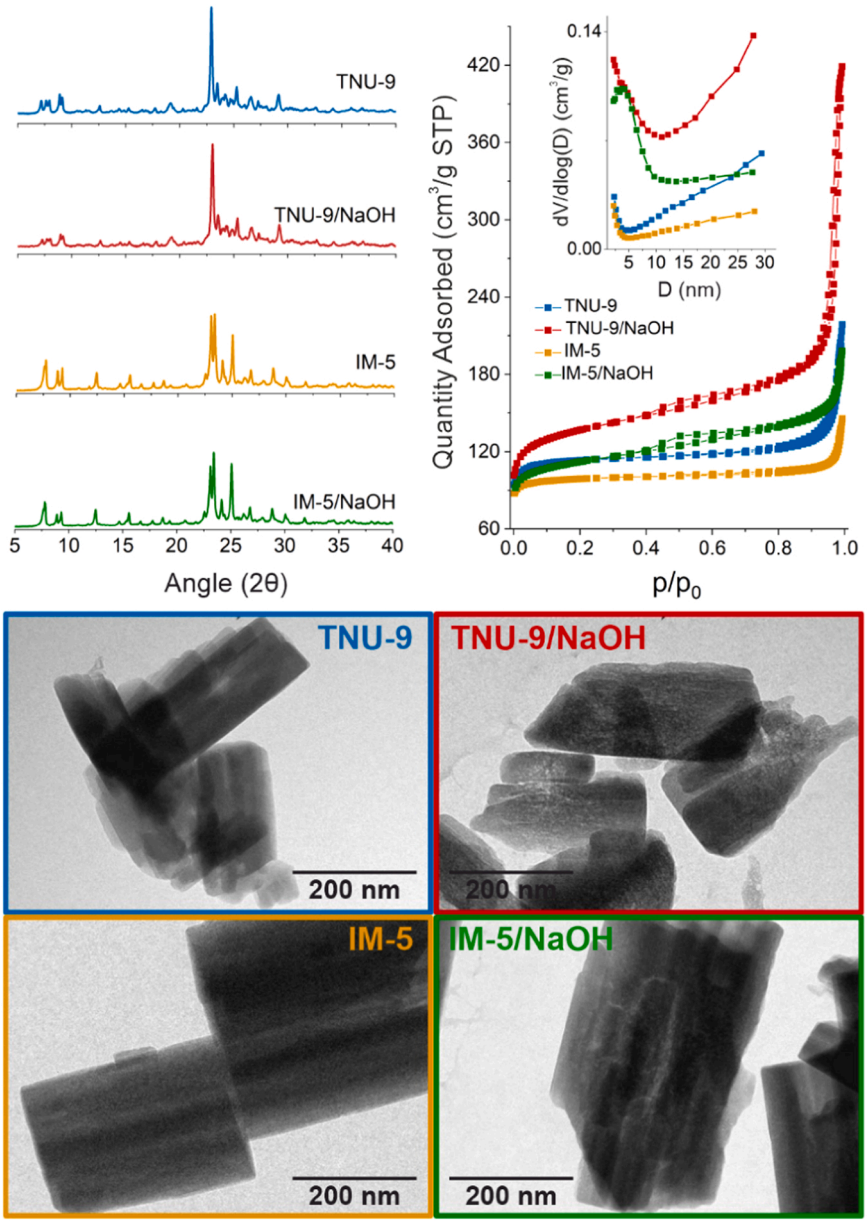

Fig. 1. The XRD patterns and adsorption-desorption isotherms of N_2 and BJH pore size distribution for native TNU-9 and IM-5 and the NaOH-treated zeolites. TEM microphotographs of the parent zeolites TNU-9 and IM-5 and the zeolites treated with NaOH.

stretching frequencies (ν_{OH}) and the $\Delta\nu_{OH.CO}$ values representing the downshift od Si(OH)Al groups band due to their involvement with hydrogen bond to CO molecule (Table 4). As a result of lowered strength of protonic sites in hierarchical zeolites the PyH^+ ions are not efficiently retained on their surface. The increase of the frequencies of the Si(OH)Al groups bands and the decrease of the $\Delta\nu_{OH\ldots CO}$ values for hierarchical materials are also indicative for the decline of the acid strength of the protonic sites after alkaline treatment. The introduction of mesoporosity in the zeolites reduces the apparent acid strength of protonic sites; they appear to be of "weaker" strength due to differences in confinement between acid sites located in the meso- and micropores. Additionally the strength of protonic sites can be inferred by the extraframework Al and silanol species in the closest vicinity [28,29]. The defect-free framework structures were identified as those promoting a higher acid strength of the intrinsic Brønsted acid sites. The decrease of Brønsted sites acid strength is the most pronounced for IM-5/NaOH zeolite. In contrast, the noticeable increase of the acid strength of Lewis sites is observed upon desilication, manifested by the increase of the $C_{Py}^{500}/C_{Py}^{170}$ values (Table 4). As mentioned earlier, the results of CO sorption further evidence the extensive production of Lewis sites in the dehydroxylation process (Fig. 2B, 2226 cm^{-1} Lewis…CO band) located on the walls of the mesopores. The strength of Lewis site increased after hierarchization what points to a high contribution of electron acceptor sites produced by dehydroxylation, as manifested by CO sorption results.

3.2.2. *Accessibility of protonic sites for molecules of various kinetic diameter*

The acid sites accessibility evaluation is helpful to standardize effectiveness of zeolites hierarachization by defining the number of sites located on mesoporous surface and micropores independently. Accessibility studies of acid sites in native and hierarchical zeolites involving quantitative FT-IR measurements with pivalonitrile (Pn, ca. 0.6 nm) and 2,6-di-*tert*-butylpyridine (dTBPy, ca. 1 nm) as probe molecules were performed [23,30]. At room temperature the diffusion of Pn in 10-ring channels is sterically limited, only the sites situated in pore entrances and on external surfaces are easily detectable by the probe. The number

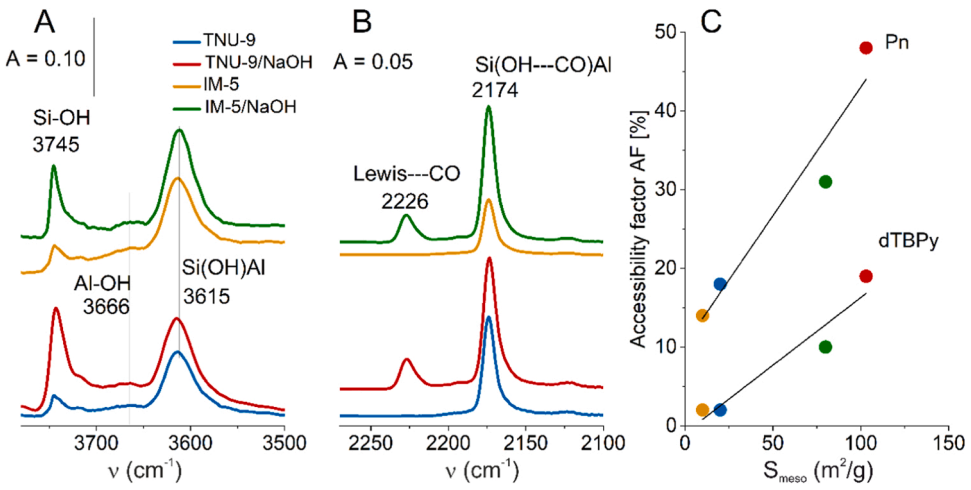

Fig. 2. FT-IR spectra (A) in the region of OH groups vibration and (B) of CO sorbed at −110 °C in parent and hierarchical zeolites. (C) Plots of accessibility factors for protonic sites (AF_B) for pivalonitrile (Pn) and 2,6-di-tert-butylpyridine (dTBPy) versus the mesopores surface area of studied zeolites.

Table 4
Acidity characteristics of the native and hierarchical zeolites: concentration of Al atoms from chemical analysis Al_{ICP}, the concentrations of Brønsted (B) and Lewis acid sites (L) from IR spectroscopy measurements with pyridine, acid strength of the Brønsted (B) and Lewis acid sites (L) achieved from the IR studies of pyridine thermal desorption ($C_{Py}^{500}/C_{Py}^{170}$), the position of the freely oscillating Si(OH)Al groups (expressed by ν_{OH} in cm^{-1}) and a low temperature shift of the Si(OH)Al groups upon CO sorption (expressed by $\Delta\nu_{OH\cdots CO}$ in cm^{-1}), accessibility factors (AF_B) for Brønsted sites derived from sorption of pivalonitrile (Pn) and 2,6-di-*tert*-butylpyridine (dTBPy).

Zeolite	Al_{ICP}	Concentration of acid sites			Acid strength of sites				AF_B	
		B	L	B + L	B $C_{Py}^{500}/C_{Py}^{170}$	L $C_{Py}^{500}/C_{Py}^{170}$	ν_{OH}	$\Delta\nu_{OH\bullet\bullet\bullet CO}$	Pn	dTBPy
	$\mu molg^{-1}$	$\mu molg^{-1}$	$\mu molg^{-1}$	$\mu molg^{-1}$	-	-	cm^{-1}	cm^{-1}	%	%
TNU-9	994	850	50	900	0.99	0.27	3617	325	18	2
TNU-9/NaOH	1280	930	210	1140	0.92	1.00	3620	310	48	19
IM-5	1180	900	100	1000	0.90	0.50	3614	328	14	2
IM-5/NaOH	1380	943	207	1150	0.73	0.95	3619	311	31	10

of Brønsted acid sites reached by Pn was achieved from the maximum intensities of the 2258 – 2278 cm^{-1} band attributed to Pn hydrogen bonded to protonic sites and its absorption coefficient (0.11 $cm^2\mu mol^{-1}$) (Table 4). Owing to kinetic diameter of ca. 1 nm the dTBPy molecules are not allowed to enter the sites in micropore entrances, thus only external sites are reached by probe [24]. The number of external protonic sites reached by dTBPy was calculated from the maximum intensity of the 1615 cm^{-1} diagnostic $dTBPyH^+$ band and its absorption coefficient (0.50 $cm^2\mu mol^{-1}$) (Table 4). The accessibility factors (AF_B) for probe molecules were defined as the number of sites detected by adsorption of Pn or dTBPy divided by the total amount of acid sites quantified by Py sorption. The effect of alkaline treatment is clearly visible as an increase of percentage of Brønsted acid sites able to react with hindered molecules. The enhanced accessibility of the sites in zeolites with secondary system of mesopores is related to the increased share of the sites exposed on the developed external surface (dTBPy sorption) and, predominantly, in pore mouths (Pn sorption) - Fig. 2C. Accessibility of protonic sites in hierarchical zeolites is the decisive factor determining their catalytic cracking properties. The protonic sites hidden inside micropores of hierarchical zeolites are more prone to react with hindered molecules when compares with sites of non-mesoporous zeolites.

The supreme Brønsted sites accessibility was found for zeolite TNU-9 treated with NaOH (Table 3, Fig. 1). The greater contribution of acid sites accessible directly from external surface (dTBPy sorption) in the total number of sites accessible, including those in pore entrances/mouths (Pn sorption) is found for TNU-9/NaOH. The treatment leads to less important enhancement of AF_B (Pn) and AF_B (dTBPy) in a case of IM-5 zeolite: as seen by the differences in the slope of linear dependency in Fig. 2C for IM-5 series. This effect might be related with limited 3D microporosity of IM-5: two 2D systems (slabs of three 2-dimensional channel systems are separated by dense framework, thus forming limited 3-dimensionality). In the IM-5/NaOH zeolite the majority of acid sites accessible to large probe molecules is located in pore mouths not on external surface.

Summing up, although the strength of protonic sites was reduced upon the alkaline treatment, their accessibility for hindered molecules became noticeably enhanced. This new picture of acidic functionality is supposed to be reflected in the catalytic cracking reactions, both employing model (*n*-decane, TiPB) and real VGO and polymer compounds (LDPE and PP) as well.

3.3. Catalytic performance in TIPB, n-decane and VGO cracking

Three different feeds: 1,3,5-tri-iso-propylbenzene (TIPB), *n*-decane and vacuum gas oil (VGO) were used in the recognition of catalytic performance of hierarchical zeolites derived from microporous TNU-9 and IM-5. The activity of zeolites in cracking of TIPB molecules, which are not able to penetrate the 10-ring channels, are expected to reveal the differences in accessibility of acid sites on the catalyst external surfaces. In contrast, the molecules of *n*-decane are able to diffuse through the system of both meso- and micropores without any hindrance thus they reach all sites offered by the zeolite. Consequently, the catalytic performance in *n*-decane cracking reactions can be addressed to intrinsic Brønsted acidity. Finally, the study is complemented by testing a real FCC feed, i.e. vacuum gas oil (VGO) which conversion requires the properly balanced acidic function of the catalyst in terms of the accessibility and strength of acid sites.

The total conversion and selectivity in TIPB cracking versus catalyst to oil ratio is presented in Fig. 3 and 1_SI. It is shown that the hierarchical zeolites offer the highest activity what is a result of the effectively developed mesopore surface area and consequently, the highest

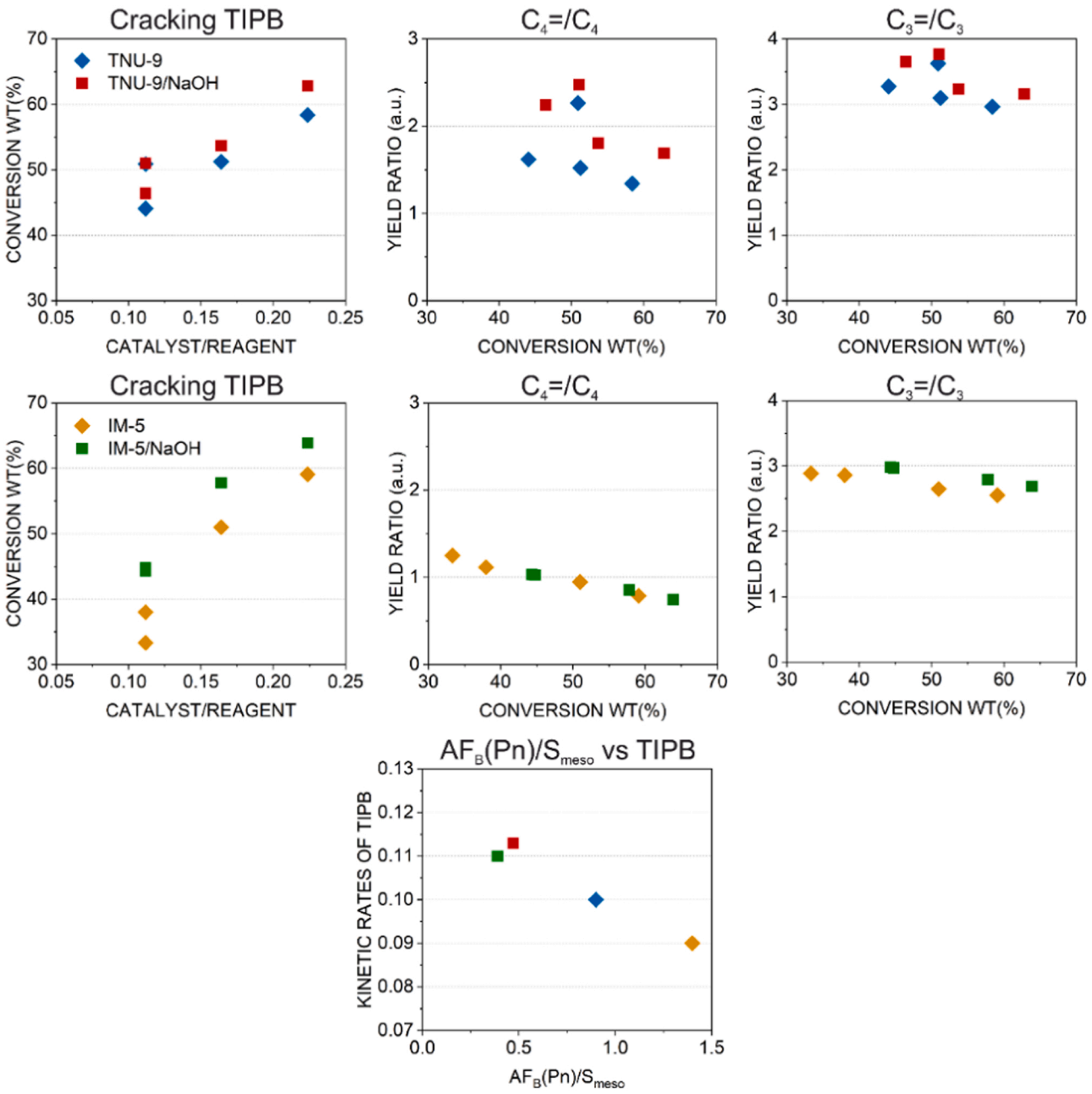

Fig. 3. Total conversion and selectivities in the cracking of TIPB at 500 °C and 60 s time on stream over parent TNU-9 and IM-5 and their hierarchical counterparts. Population of protonic sites on mesopore surface ($AF_B(Pn)/S_{meso}$) as a linear function of kinetic rates of TIPB cracking.

accessibility of protonic sites to the bulky TIPB molecules. This effect is particularly seen for IM-5/NaOH material. The zeolite IM-5 has a 2D 10-ring channel system with effective pore diameter ranging from 4.8 to 5.5 Å. The unusual feature of IM-5 zeolite is that its channel system also has a limited third dimension as three 2D channel systems are connected to one another giving a ~2.5-nm thick pore system (nanoslab) separated by single walls. It gives IM-5 the character of a 3D channel system with complex intersections while retaining the overall effect of a 2D one with long-range diffusion restricted to just two dimensions. The NaOH treated samples presents somewhat higher olefinicity in the C_3 and C_4 fractions ($C_{3=}/C_3$, $C_{4=}/C_4$) since the primary reactions on the surface are beneficial. Propylene ($C_{3=}$) is a primary product in the dealkylation of TIPB, while ethylene ($C_{2=}$) and propane (C_3) are secondary from oligomerization-cracking and hydrogen transfer processes, respectively. Attaining ethylene by oligomerization-cracking requires the formation of an unstable primary carbocation and the presence of strong acid sites and/or narrow pores and, finally, the severe reaction conditions. The importantly reduced acid strength of Brønsted sites and the development of mesoporosity at the expense of microporous environment do not provide the conditions for very demanding oligomerization-cracking reaction and justifies lower selectivity of IM-5/NaOH to dry gas while for TNU-9/NaOH, which kept the sites of high strength, the amount of dry gases is preserved on the level of native TNU-9 material. These results confirm that the enhanced mesoporosity (Table 3) beneficial for the increased accessibility for TIPB molecules does not compensate considerably lowered strength of Brønsted acid sites (Table 4). The dependence of the kinetic rate constants referred to $AF_B(Pn)$ (Fig. 3) clearly show that increased population of protonic sites on the surface, expressed as $AF_B(Pn)/S_{meso}$ benefit to the catalytic activity. Still however, the contribution of silanols, which are highly populated in mesoporous zeolites, has to be taken into account.

In contrast, the zeolites catalytic performance in *n*-decane cracking

reactions can be correlated with the intrinsic Brønsted acidity defined as the number and the strength of acid sites in micropores (Fig. 4). All the spectral signatures describing the strength of Brønsted acid sites, i.e. $C_{Py}^{500}/C_{Py}^{170}$, ν_{OH}, $\Delta\nu_{OH\bullet\bullet\bullet CO}$, linearly correlate with the kinetic rate constants (Fig. 4 and 2_SI). The purely microporous catalysts possess the strongest protonic sites (Table 4) thus they provide the highest catalytic activity. Alkaline leaching, resulting in the lowering of the Si(OH)Al groups averaged strength, reduces also the activity of hierarchical zeolites for *n*-decane cracking. Again, the lowest strength of sites in IM-5/NaOH is reflected in the most important decrease of *n*-decane conversion. Interestingly, the correlation with the strength of sites determined from Py-thermodesorption studies ($C_{Py}^{500}/C_{Py}^{170}$) is weaker than for the acidity signatures (ν_{OH}, $\Delta\nu_{OH\bullet\bullet\bullet CO}$) directly referred to bridging hydroxyls, i.e. Si(OH)Al. To explain this phenomenon the realumination process has to be recalled as decisive for the formation of Brønsted and Lewis sites on the mesopore surface. The IR spectroscopic studies have proved the existence of protonic sites situated on mesoporous surface but not represented by the Si(OH)Al groups due to the Al-atoms reinsertion during desilication process [31,32]. For instance, in NaOH-treated zeolite ZSM-5 the majority of the protonic sites was found not to contribute to the Si(OH)Al band at ca. 3615 cm^{-1}; additionally these sites are of weaker acid strength than typical zeolitic Si(OH)Al groups [22]. A linear dependence of the kinetic rate constants on the acid strength of the Si(OH)Al groups (identified by the ν_{OH} and $\Delta\nu_{OH\bullet\bullet\bullet CO}$ values) evidences the dominant role of bridging hydroxyls located in micropores over hydroxyls populated on external surfaces in *n*-decane cracking. Still however, the significant input of shortened diffusion path thus exposing of the intrinsic Si(OH)Al sites to *n*-decane molecules is manifested as the linear correlation between $AF_B(Pn)/S_{meso}$ and the kinetic rate constants (Fig. 4).

Catalytic activity tests of the cracking of vacuum gas oil (Fig. 5), a feed with reagents of various degrees of branching, requires comprehensive set of parameters as high specific surface area of both micro-and mesopores and the proper acidic function. The potential application of

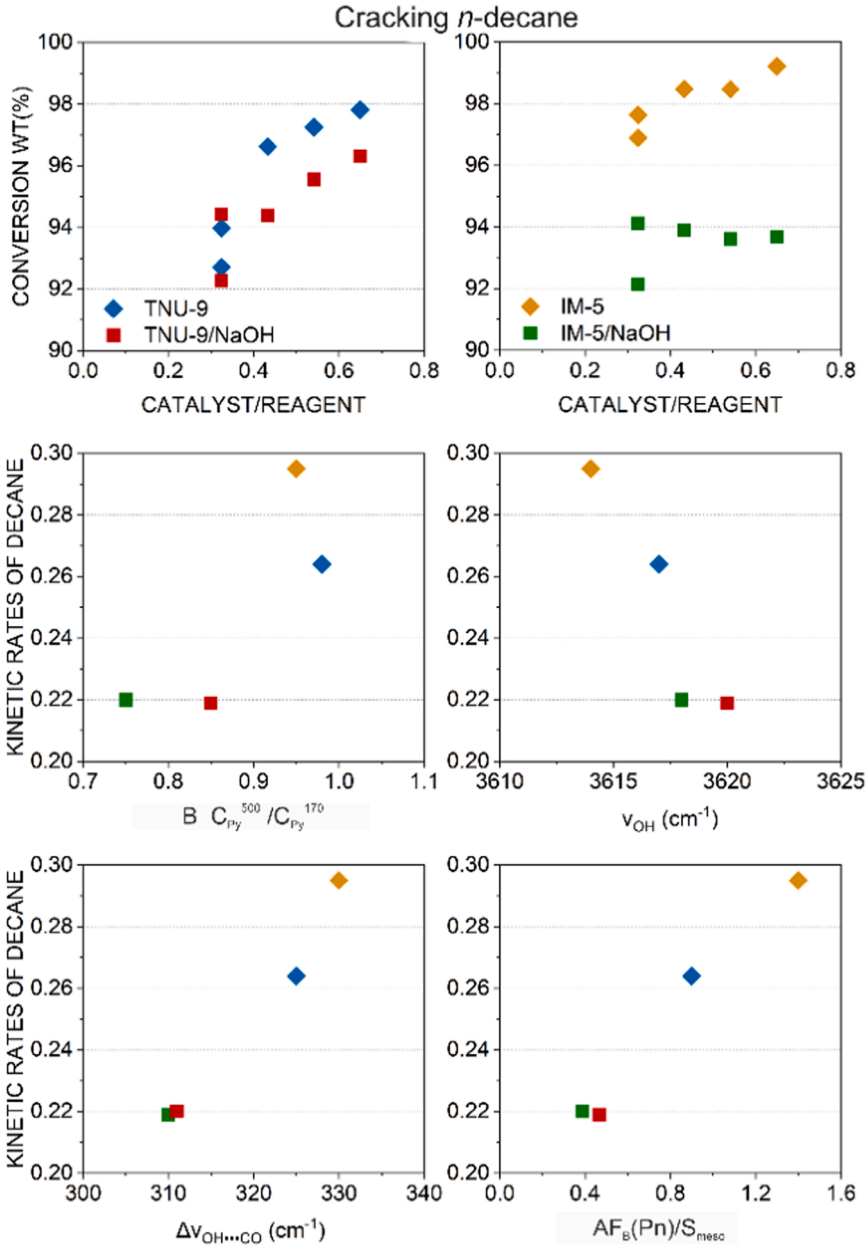

Fig. 4. Total conversion in the cracking of n-decane at 500 °C and 60 s time on stream over parent TNU-9 and IM-5 and their hierarchical counterparts supplemented with the acidity parameters of Brønsted sites ($C_{Py}^{500}/C_{Py}^{170}$, ν_{OH}, $\Delta\nu_{OH\bullet\bullet\bullet CO}$, $AF_B(Pn)/S_{meso}$,) correlated with kinetic rate constants of n-decane cracking.

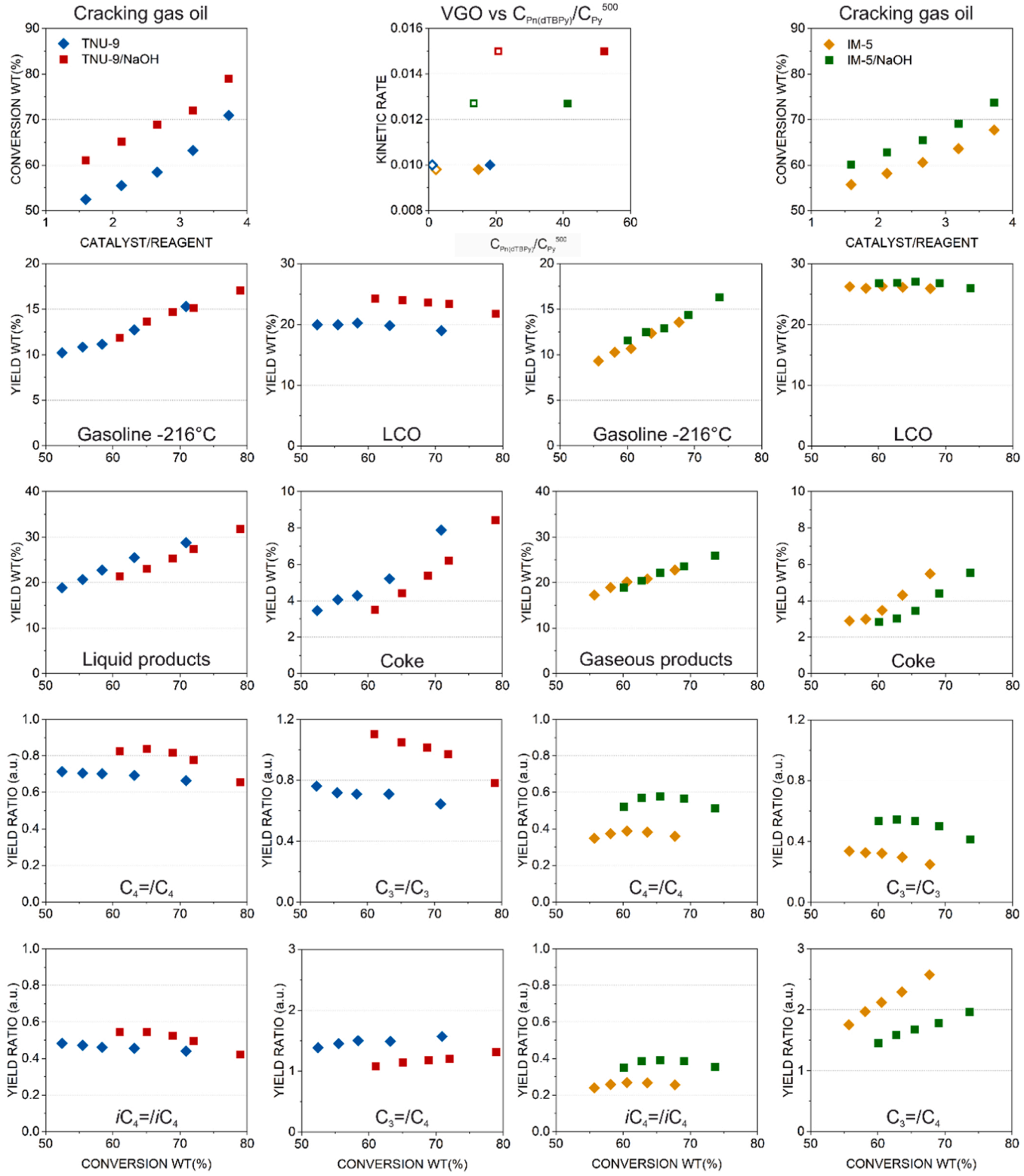

Fig. 5. Total conversion and selectivities in the cracking of vacuum gas oil at 520 °C and 30 s time on stream over parent TNU-9 and IM-5 and their hierarchical counterparts. The dependence of catalytic kinetic rates of vacuum gas cracking on the share of strong protonic sites accessible for Pn (solid symbols) and dTBPy (open symbols) for native TNU-9 and IM-5 and hierarchical zeolites ($C_{Pn(dTBPy)}/C_{Py}^{500}$).

hierarchical TNU-9/NaOH and IM-5/NaOH zeolites in gas oil cracking process was evaluated. The hierarchical zeolites for the cracking of vacuum gasoil give the 10–18% higher conversions than the conversions obtained with purely microporous counterparts (Fig. 5). The weaker acid strength of protonic sites is balanced by their highly enhanced accessibility related to the mesopore system (Fig. 5). For further considerations, the number of protonic sites accessible for bulky Pn and dTBPy molecules was faced with the concentration of Brønsted sites able to retain the pyridine molecules at the VGO cracking temperature (C_{Pn}/C_{Py}^{500}) – Table 4. A linear dependence of second-order kinetic rate

constants for vacuum gas oil cracking on the C_{Pn}/C_{Py}^{500} parameter (Fig. 5) clearly shows that catalytic activity is mutually dependent on the number of both the highest strength protons and those easily available from external surface. Since mesoporosity fabrication always leads to increased share of protonic sites of lower strength maintaining of the high VGO conversion level requires an appropriate balance between the strength of intrinsic protonic sites and their accessibility.

The advantage of hierarchical zeolites over both microporous counterparts is also documented by the higher selectivity towards the desired LCO fraction accompanied by lower coke content. The production of gasoline is beneficially maintained at the same level in microporous and hierarchical zeolites. More differences are observed in the olefinicity ratios. The enhanced accessibility of the protonic sites reduced hydrogen transfer as secondary reactions that consume olefins. In fact, the hierarchical zeolites provide the shorter reaction path for reagents, offering the highest olefinicity in the C_3 and C_4 fraction (see Fig. 9 for $C_{3=}/C_3$,$C_{4=}/C_4$, $iC_{4=}/iC_4$ ratios) and producing less coke and dry gases. The studies of hierarchical zeolites with regard to gasoil cracking are mainly devoted to the fabrication of the catalyst that improve propylene yields along with an increase LCO selectivity [33]. Desilication process makes the IM-5 structure more open (forcing the connection between the nanoslabs) thus the relative catalytic effects (highest olefinicity in the C_3 and C_4 fraction, less coke and dry gases) related to generated mesoporsity are more pronounced for this structure than for TNU-9 of typical 3D structure.

3.4. Catalytic PP and LDPE cracking: thermogravimetric and operando FT-IR-GC-MS studies

The applicability of hierarchical TNU-9 and IM-5 in the cracking reactions of polypropylene and low density polyethylene was also investigated. Kinetic diameter of polymers is greatly larger than the 10-ring pore entrance in the TNU-9 and IM-5 zeolites therefore catalytic degradation of polymers is initiated over the active sites on the external surface of the zeolite crystals. Then, the partially degraded products which are able to diffuse into the micropores of the zeolite are cracked at the pore entrance and/or on the acid sites located inside the micropores. Consequently, efficiency of preliminary cracking reactions can be correlated with the number of acid sites situated on the mesopore surface and pore entrances while the sites hidden inside the micropores provide a relevant input to the cracking reaction selectivity. The results of PP and LDPE catalytic cracking over the native and hierarchical zeolites as a function of temperature are presented in Fig. 6. The cracking of PP over the studied zeolites required lower temperatures than for LDPE, what can be associated with the branched character (the presence of large number tertiary carbon) of the PP chain structure. The branching facilitates the formation of tertiary carbocations what positively affects PP susceptibility to the cracking reactions. The conversion curves both LDPE and PP are shifted to lower temperatures for the hierarchical TNU-9/NaOH with respect to the microporous parent zeolite.

For PP temperatures for 50% and 75% conversions ($T_{50\%}$ and $T_{75\%}$)

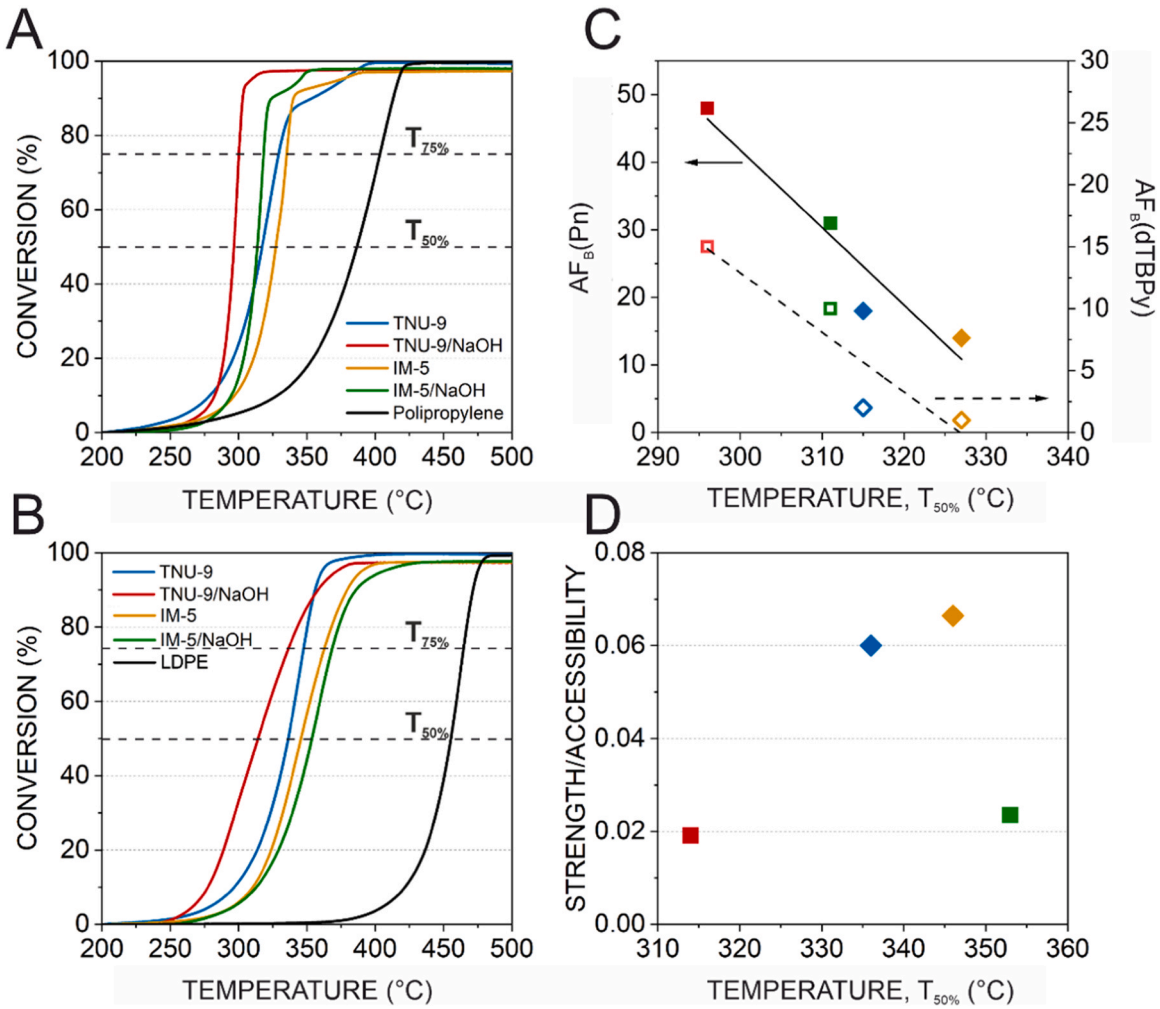

Fig. 6. Results of PP (A) and LDPE (B) catalytic cracking conversion as a function of temperature over the microporous and hierarchical zeolites TNU-9 and IM-5. (C) Temperatures for 50% conversion ($T_{50\%}$) for PP against the accessibility factor values (AF) for the Brønsted acid sites estimated from Pn (AF_B(Pn)) and dTBPy (AF_B(dTBP)) sorption experiments and (D) Temperatures for 50% conversion ($T_{50\%}$) for LDPE cracking plotted against the (C_{Py}^{500} /C_{Py}^{170})/ AF_B(Pn).

over zeolites are about 80 °C lower than of thermal cracking. Among microporous materials the highest activity is found for TNU-9 what correlates with higher accessibility of protonic sites in this structure. The alkaline leaching further improves the catalytic behavior of both TNU-9/NaOH and IM-5/NaOH, still the highest enhancement in catalytic activity is observed for mesoporous zeolite TNU-9/NaOH. At higher temperatures (300–375 °C) the course of the conversion curve for IM-5/NaOH clearly indicates the beneficial influence of the secondary mesoporosity on the reduced carbonaceous species formation. This effect is even more visible for TNU-9/NaOH. From the slope of conversion curves for PP the improvement in catalytic performance due to a lower coking of the hierarchical catalyst can be concluded. The reduction of $T_{50\%}$ and $T_{75\%}$ is not very significant for hierarchical materials compared to microporous ones because the branched character of PP makes the cracking reactions very efficient over even slightly acidic external silanols. Undeniably, the linear dependence of $T_{50\%}$ and $T_{75\%}$ on the accessibility factor for Pn is observed for all the materials. These corroborate well with TIPB cracking results where the improvement of accessibility of sites more positively influenced the catalytic performance of hierarchical TNU-9/NaOH than IM-5/NaOH. The improvement in catalytic performance for hierarchical counterparts was also observed in VGO cracking.

The LDPE is less susceptible for the cracking, still however the activity trend was kept in TNU-9 series. The alkaline leaching, however, negatively affects the IM-5/NaOH catalytic performance: the non-leached native IM-5 appeared as the most active. It suggests that the cracking of LDPE is more influenced by the strength of acid sites than by their accessibility. After desilication, the strength of Brønsted acid sites was reduced in both hierarchical zeolites, however, for IM-5/NaOH it is a two-fold decrease comparing with TNU-9/NaOH. Therefore, IM-5/NaOH does not follow the linear trend of the dependence of $T_{50\%}$ and $T_{75\%}$ on the parameters describing the acid strength. These observation are further supported by *n*-decane cracking results, the activity loss is more noticeable for IM-5/NaOH zeolite than for TNU-9/NaOH accommodating protonic sites of higher strength. The acidity has proven to rule the activity of also commercial FCC catalysts in high density polyethylene cracking, the higher the concentration and strength of acid sites the higher was the activity [34].

Operando FT-IR studies were performed on microporous TNU-9 and its hierarchical TNU-9/NaOH as the most active catalysts in the thermogravimetric studies. Both in PP and LDPE cracking processes the microporous TNU-9 provided higher cracking efficiency with higher amounts of light hydrocarbons (C_4-C_5, similar fraction of C_3 products) whereas the mesoporous analogue gave higher amounts of liquid

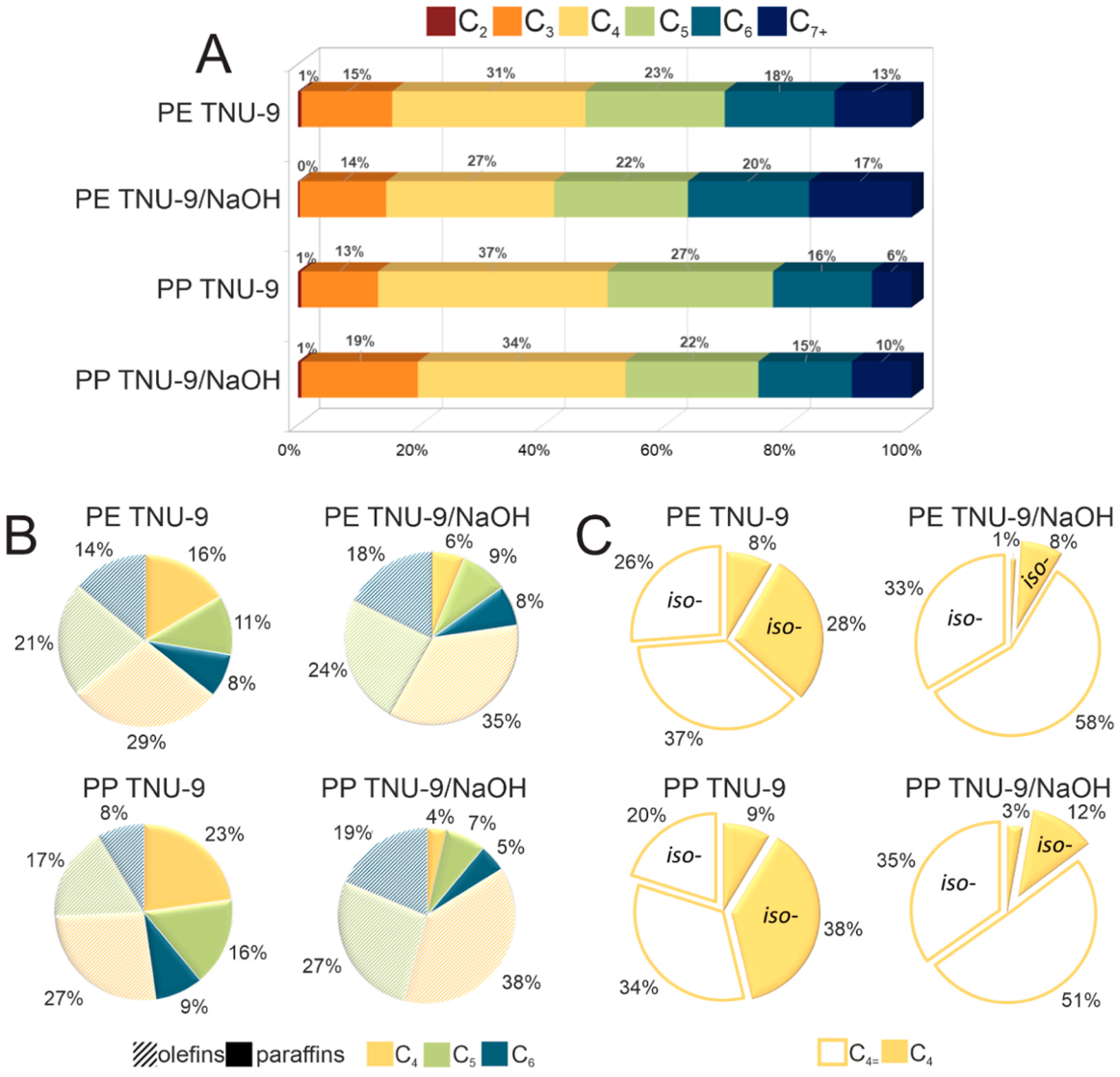

Fig. 7. Microporous and hierarchical zeolites TNU-9 in LDPE and PP catalytic cracking: (A) distribution of the cracking products: selectivities; the share (%) of the paraffin and olefin fractions (B) and the share of the branched and linear compounds (C) in C_4 fraction.

fraction (C_6-C_{7+}). The microporous TNU-9 zeolite favored secondary recracking reactions over acid sites of high strength. In the case of hierarchical TNU-9 zeolite the primary products leave the micropores rapidly due to lack of diffusional constraints [35–37]. Among polymers cracking products (Fig. 7) higher share of unsaturated hydrocarbons (olefins mainly) was found for zeolite TNU-9/NaOH due to hydride transfer (HT) processes [38] facilitated by both the presence of additional mesopore system and higher density of acid sites (Table 4). The formation of olefins is more noticeable in PP then LDPE cracking due to easier formation of high number of branched carbonations. Highly developed mesoporous surface area and vastly populated and accessible Brønsted sites in TNU-9/NaOH offered also the highest olefinicity in the C_3 and C_4 fraction (see Fig. 5 for $C_{3=}/C_3$,$C_{4=}/C_4$, $iC_{4=}/iC_4$ ratios) in VGO cracking reaction.

Bimolecular hydride-transfer reactions can be also enhanced by the presence of huge amount of silanol groups in mesoporous zeolite that can help to retain the adsorbate molecules (Fig. 2A). Besides proton donor acid sites, electron acceptor Lewis sites highly populated in TNU-9/NaOH (Table 4) should be considered to participate in secondary HT processes [39]. The lowered acid strength of protonic sites is believed to facilitate the carbocations desorption from the Brønsted acid sites and therefore improve the share of *iso*-olefins for hierarchical zeolite. As aforementioned, the TNU-9/NaOH zeolite produced less coke and dry gases in VGO cracking while opposite is found for LDPE and PP cracking. The catalyst deactivation by pore blockage is also decisive parameter in polymer catalytic cracking [37,40,41]. The similar behavior was found for commercial equilibrated FCC catalysts when HDPE was added to VGO feed. The coking of micropores was increased in the presence of polymer in the feed, the micropores were preferable location for coke [42]. It is worth noting that the TNU-9/NaOH hierarchical zeolite, compared to the ZSM-5 catalysts of bigger external surface area [43], is characterized by much higher activity and selectivity to C_4 and C_5 fractions in cracking of LDPE.

Additional insight into the cracking of LDPE and PP over surface of TNU-9 zeolite samples was given by 2D COS (two-dimensional correlation) analysis of FT-IR spectra collected during reaction (Fig. 8). The 2D COS analysis [44] is a mathematical approach offering the scrutiny of the dynamic spectra collated during an external perturbation, in this case the time of cracking reaction. The analysis can be performed in both synchronous and asynchronous modes, while former provides information on the simultaneous or coincident changes, the latter one formulates the sequential order of spectral intensity changes at given ν_1 and ν_2. The strong correlation found for the CH_3 deformation (1400–1350 cm^{-1}) and stretching (2970, 2968 cm^{-1}) bands points to end-chain cracking mechanism of polymers and higher share of paraffinic products formed over TNU-9. Additionally, for the TNU-9/NaOH stronger correlations are found for CH_2 (2925, 2855 cm^{-1}) representative bands, thus the higher acid sites accessibility offers the middle-chain cracking mechanism followed by formation of olefins. Further, the correlation of complex C═C stretching bands (1515 – 1480 cm^{-1}) and C-H stretching bands region is distinguished importantly for TNU-9/NaOH, thus higher olefinicity of products is expected and indeed found (Fig. 7) for this sample. The high share of branched hydrocarbons in PP cracking products, especially for TNU-9, is a consequence of correlations between the C═C stretching bands (1515 – 1480 cm^{-1}) and both the CH_3 and CH_2 stretching bands (3000 – 2800 cm^{-1}). Nevertheless, only week correlation for bands above 1505 cm^{-1} are found and this region might be subscribed to bands representative for coke precursors. For TNU-9/NaOH sample the formed olefins represented by C═C stretching (1515 – 1480 cm^{-1}) and CH_2 deformation (1380 – 1430 cm^{-1}) bands are preferentially desorbed from catalysts surface before the C-H stretching (3000 – 2800 cm^{-1}) bands intensity decreases. Thus before the cracking reaction further proceeds the light olefins are desorbed from catalysts surface. The coke precursors retain on surface as the bands in region above 1505 cm^{-1} are altered only after the C-H stretching (3000 – 2800 cm^{-1}) bands intensity decrease.

The enhanced density of acid sites and external silanols supported by intracrystalline mesoporosity induces the coking phenomenon by facilitating secondary successive reactions (oligomerization, condensation, and hydrogen transfer processes). The coking process can be easily confirmed by the complex IR band around 1650–1500 cm^{-1} (Fig. 9). It is well seen that the type of the coke species accumulated on the zeolite surface is dependent on the both type of the polymer and the presence of secondary mesoporosity. The PP cracking and lack of mesoporous characteristic resulted in less fouled catalysts, in line with TGA data (Table 5). The carbonaceous adsorbed species are characterized by the IR bands located at 1565 cm^{-1} and 1595 cm^{-1} which allow to identify the coke species as conjugated olefinic species and hydrogen-deficient polyaromatic species [45], respectively. Among of the coke precursors also 1,2,4-trimethylbenzene was identified (1505 cm^{-1}). While in TNU-9 mainly conjugated olefinic species serve as coke compounds formed due to LDPE cracking, in its mesoporous counterpart the polyaromatics species are detected as the most populated coke compounds. Also PP cracking-originated coke species are more abundant in conjugated olefins in TNU-9 than in TNU-9/NaOH. The coke burning in TNU-9/NaOH is initiated over the hydrogen atoms in the aliphatic units when aromatic ones are oxidized in the next order which is detected in IR spectra as the erosion of the CH_3 and CH_2 deformation bands followed by the removal of 1565–1595 cm^{-1} complex band. In microporous zeolite coke combustion is more progressed at lower temperature than in hierarchical counterpart due to the higher abundance of the external surface olefinic species, as also confirmed by lower CO_2/H_2O ratio for purely microporous zeolite.

To sum up, the 10-ring topologies (MFI, IMF, TUN) with secondary mesoporosity follows the same trend both in TIBP an *n*-decane cracking. Hierarchization benefits the activity for bulky reagent (TIPB) while it is detrimental in *n*-decane cracking performance. Due to the highest volume of internal cavities TNU-9 zeolite is the most susceptible for coking.

4. Conclusion

This study highlights the applicability of a well-adjusted desilication with NaOH to the formation of zeolites with combined mesoporosity and microporosity and preserved the intrinsic acidity of the parent zeolite. Detailed characterization of the samples documented that hierarchical TNU-9 increased yields to LCO and propylene during gas–oil cracking reaction. The porosity, and acid sites strength related to confinement were also found to play complementary roles in a model polyethylene and polypropylene cracking providing among products a bigger share of *iso*-olefins. The mesoporous TNU-9 is therefore an excellent example for the possibility of designing catalyst dedicated to the chemical recycling of PP and LDPE polymers in the FCC process.

Author contributions

KGM was the originator of the concept and planned and supervised the experiments. SV and JMT supervised the pristine material syntheses and cracking reactions involving gas oil, *n*-decane, and TIPB. KW undertook the characterization of acidic properties of the materials with the FT-IR. KAT was responsible for the pristine material syntheses and hierarchization, the cracking reactions performing (gas oil, *n*-decane, TIPB), and operando FT-IR and UV–VIS results interpretation. KGM and KT wrote and edited the final manuscript. F.R. participated in the preparation of the final manuscript version. All authors have read and agreed to the published version of the manuscript.

Declaration of Competing Interest

The authors declare that they have no known competing financial interests or personal relationships that could have appeared to influence the work reported in this paper.

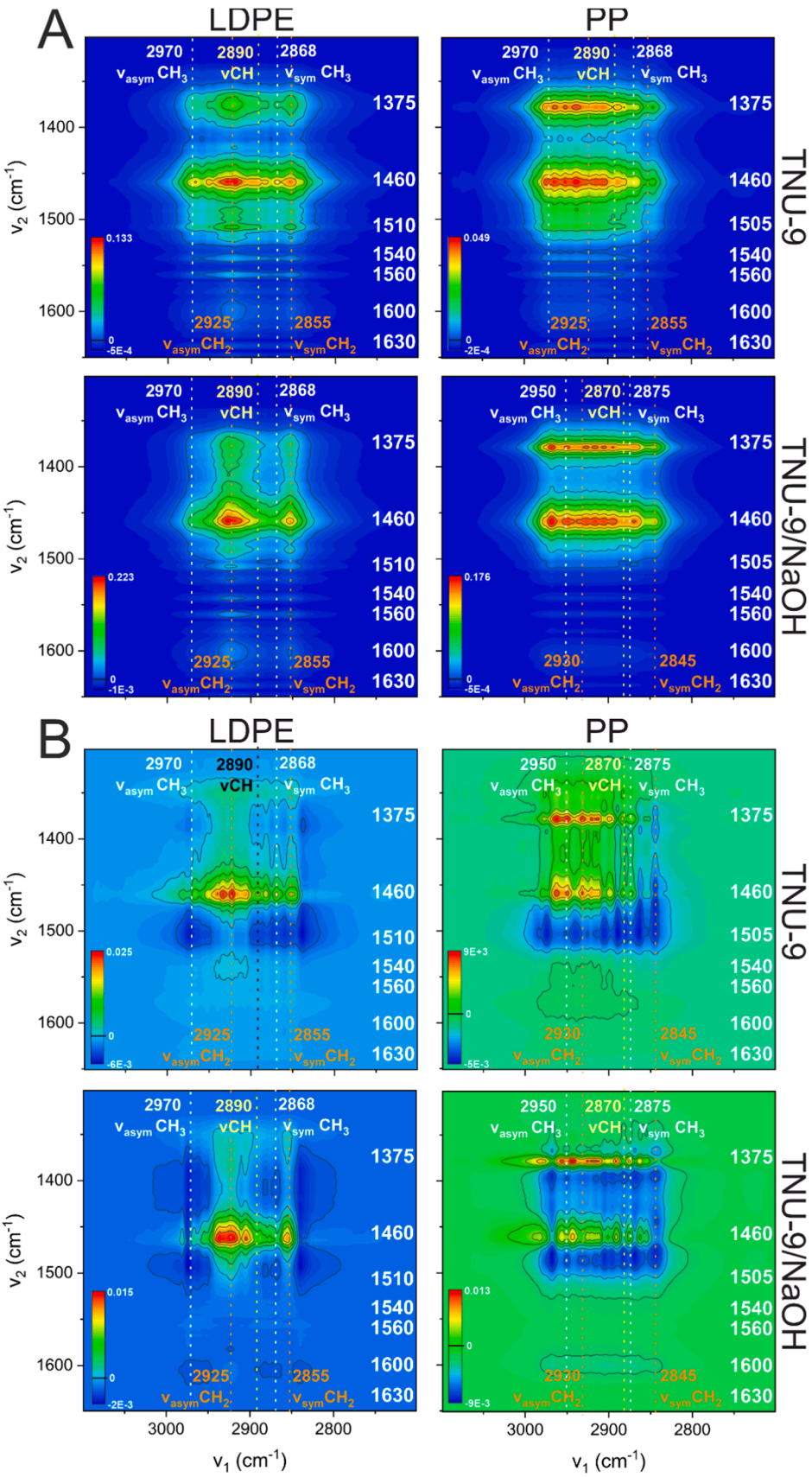

Fig. 8. 2D COS maps of FT-IR spectra registered during LDPE and PP cracking in (A) synchronous and (B) asynchronous mode for TNU-9 and TNU-9/NaOH samples.

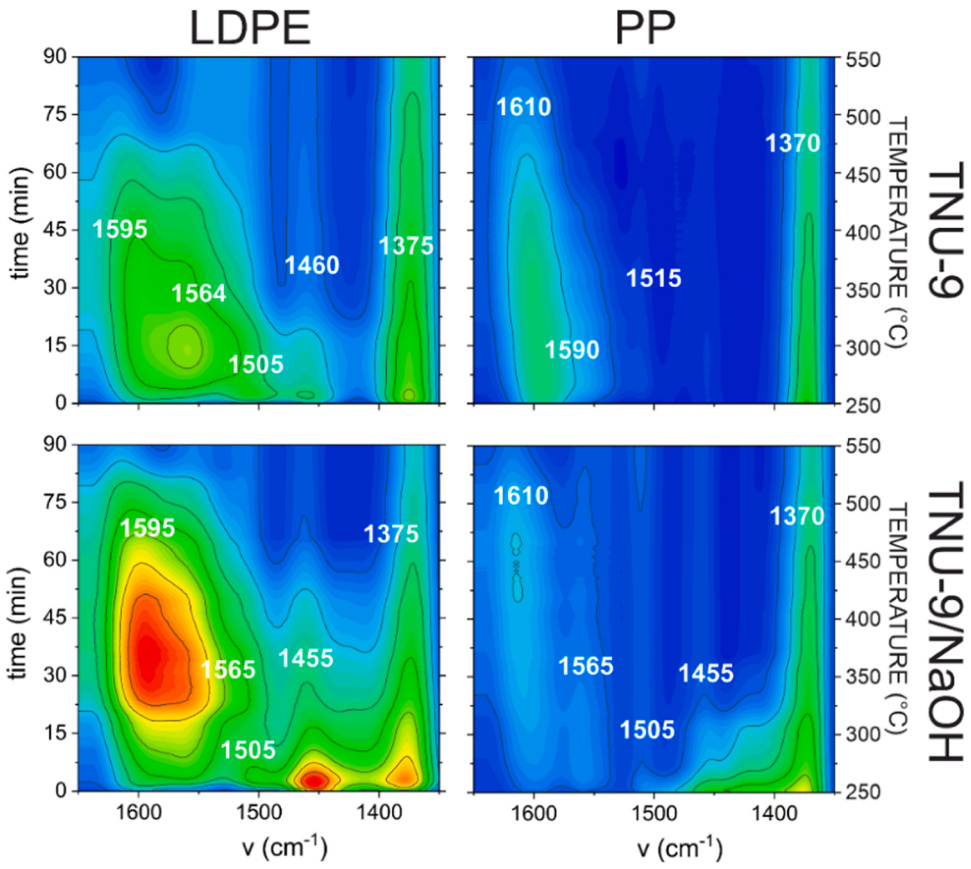

Fig. 9. FT-IR characteristics of coke species removal from microporous and hierarchical zeolites TNU-9 by burning off in air.

Table 5
TGA analysis of the content of coke formed during LDPE and PP cracking.

Zeolite	TNU-9	TNU-9/NaOH	IM-5	IM-5/NaOH
Coke % LDPE	7.4	10.2	3.0	6.5
Coke % PP	3.3	7.4	2.7	7.1

Data availability

Desilicated TNU-9 and IM-5 in cracking processes (Original data) (Jagiellonian University Repository)

Acknowledgments

KGM acknowledges the Grant No 2021/43/B/ST4/00307 form National Science Center, Poland. KAT acknowledges the Grant No 2020/37/B/ST4/01215 form National Science Center, Poland. For the purpose of Open Access, the author has applied a CC-BY public copyright licence to any Author Accepted Manuscript (AAM) version arising from this submission. JMT acknowledges the Grant MFA/2022/016 from Advanced Materials program supported by MCIN with funding from European Union NextGenerationEU (PRTR-C17. I1) and by Generalitat Valenciana. The study was carried out using research infrastructure purchased with the funds of the European Union in the framework of the Smart Growth Operational Program, Measure 4.2; Grant No. POIR.04.02.00-00-D001/20-00, "ATOMIN 2.0 - ATOMic scale science for the INnovative economy". The open-access publication of this article has been supported by a grant from the Faculty of Chemistry under the Strategic Programme Excellence Initiative at Jagiellonian University.

References

[1] Y. Wang, Y. Zhang, H. Fan, P. Wu, M. Liu, X. Li, J. Yang, C. Liu, P. Bai, Z. Yan, Elucidating the structure-performance relationship of typical commercial zeolites in catalytic cracking of low-density polyethylene, Catal. Today 405–406 (2022) 135–143.
[2] R. Palos, A. Gutiérrez, F.J. Vela, M. Olazar, J.M. Arandes, J. Bilbao, Waste refinery: the valorization of waste plastics and end-of-life tires in refinery units. a review, Energy Fuels 35 (2021) 3529–3557.
[3] G. Elordi, M. Olazar, P. Castaño, M. Artetxe, J. Bilbao, Polyethylene cracking on a spent FCC catalyst in a conical spouted bed, Ind. Eng. Chem. Res. 51 (2012) 14008–14017.
[4] R.C. Mordi, R. Fields, J. Dwyer, Thermolysis of low density polyethylene catalysed by zeolites, J. Anal. Appl. Pyrolysis 29 (1994) 45–55.
[5] R. Bagri, P.T. Williams, Catalytic pyrolysis of polyethylene, J. Anal. Appl. Pyrolysis 63 (2002) 29–41.
[6] P. Castaño, G. Elordi, M. Olazar, A.T. Aguayo, B. Pawelec, J. Bilbao, Insights into the coke deposited on HZSM-5, Hβ and HY zeolites during the cracking of polyethylene, Appl. Catal. B Environ. 104 (2011) 91–100.
[7] K.A. Tarach, K. Pyra, S. Siles, I. Melián-Cabrera, K. Góra-Marek, Operando study reveals the superior cracking activity and stability of hierarchical ZSM-5 catalyst for the cracking of low-density polyethylene, ChemSusChem 0 (2018).
[8] Y.-H. Seo, K.-H. Lee, D.-H. Shin, Investigation of catalytic degradation of high-density polyethylene by hydrocarbon group type analysis, J. Anal. Appl. Pyrolysis 70 (2003) 383–398.
[9] K. Pyra, K.A. Tarach, D. Majda, K. Góra-Marek, Desilicated zeolite BEA for the catalytic cracking of LDPE: the interplay between acidic sites' strength and accessibility, Catal. Sci. Technol. 9 (2019) 1794–1801.
[10] J.S. Buchanan, The chemistry of olefins production by ZSM-5 addition to catalytic cracking units, Catal. Today 55 (2000) 207–212.
[11] M.A. den Hollander, M. Wissink, M. Makkee, J.A. Moulijn, Gasoline conversion: reactivity towards cracking with equilibrated FCC and ZSM-5 catalysts, Appl. Catal. A Gen. 223 (2002) 85–102.
[12] J.M. Arandes, J. Ereña, J. Bilbao, D. López-Valerio, G. de la Puente, Valorization of the blends polystyrene/Light cycle oil and polystyrene–butadiene/light cycle oil over HZSM-5 zeolites, Ind. Eng. Chem. Res. 42 (2003) 3700–3710.
[13] A.I. Hussain, A.M. Aitani, M. Kubů, J. Čejka, S. Al-Khattaf, Catalytic cracking of Arabian Light VGO over novel zeolites as FCC catalyst additives for maximizing propylene yield, Fuel 167 (2016) 226–239.
[14] K.A. Tarach, K. Góra-Marek, J. Martinez-Triguero, I. Melián-Cabrera, Acidity and accessibility studies of desilicated ZSM-5 zeolites in terms of their effectiveness as

catalysts in acid-catalyzed cracking processes, Catal. Sci. Technol. 7 (2017) 858–873.
[15] K.A. Tarach, J. Martinez-Triguero, F. Rey, K. Gora-Marek, Hydrothermal stability and catalytic performance of desilicated highly siliceous zeolites ZSM-5, J. Catal. 339 (2016) 256–269.
[16] A. Marcilla, A. Gómez-Siurana, F. Valdés, Catalytic cracking of low-density polyethylene over H-Beta and HZSM-5 zeolites: Influence of the external surface. kinetic model, Polym. Degrad. Stab. 92 (2007) 197–204.
[17] L.O. Mark, M.C. Cendejas, I. Hermans, The use of heterogeneous catalysis in the chemical valorization of plastic waste, ChemSusChem 13 (2020) 5808–5836.
[18] R. Aguado, R. Prieto, Ma.J.S. José, S. Alvarez, Mn Olazar, J. Bilbao, Defluidization modelling of pyrolysis of plastics in a conical spouted bed reactor, Chem. Eng. Process. Process.Intensif. 44 (2005) 231–235.
[19] S.B. Hong, H.-K. Min, C.-H. Shin, P.A. Cox, S.J. Warrender, P.A. Wright, Synthesis, crystal structure, characterization, and catalytic properties of TNU-9, J. Am. Chem. Soc. 129 (2007) 10870–10885.
[20] E. Benazzi, J. Guth, L. Rouleau, Preparation of IM-5 zeolite and its catalytic applications, PCT Int. Appl. 98 (1998) 17581.
[21] A. Corma, A. Chica, J.M. Guil, F.J. Llopis, G. Mabilon, J.A. Perdigón-Melón, S. Valencia, Determination of the pore topology of zeolite IM-5 by means of catalytic test reactions and hydrocarbon adsorption measurements, J. Catal. 189 (2000) 382–394.
[22] K. Sadowska, K. Gora-Marek, J. Datka, Hierarchic zeolites studied by IR spectroscopy: acid properties of zeolite ZSM-5 desilicated with NaOH and NaOH/tetrabutylamine hydroxide, Vib. Spectrosc. 63 (2012) 418–425.
[23] K. Sadowska, K. Gora-Marek, J. Datka, Accessibility of acid sites in hierarchical zeolites: quantitative IR studies of pivalonitrile adsorption, J. Phys. Chem. C. 117 (2013) 9237–9244.
[24] K. Gora-Marek, K. Tarach, M. Choi, 2,6-Di-tert-butylpyridine sorption approach to quantify the external acidity in hierarchical zeolites, J. Phys. Chem. C. 118 (2014) 12266–12274.
[25] D. Verboekend, M. Milina, S. Mitchell, J. Pérez-Ramírez, Hierarchical zeolites by desilication: occurrence and catalytic impact of recrystallization and restructuring, Cryst. Growth Des. 13 (2013) 5025–5035.
[26] F. Bleken, W. Skistad, K. Barbera, M. Kustova, S. Bordiga, P. Beato, K.P. Lillerud, S. Svelle, U. Olsbye, Conversion of methanol over 10-ring zeolites with differing volumes at channel intersections: comparison of TNU-9, IM-5, ZSM-11 and ZSM-5, Phys. Chem. Chem. Phys. 13 (2011) 2539–2549.
[27] K. Sadowska, K. Gora-Marek, M. Drozdek, P. Kustrowski, J. Datka, J. Martinez Triguero, F. Rey, Desilication of highly siliceous zeolite ZSM-5 with NaOH and NaOH/tetrabutylamine hydroxide, Microporous Mesoporous Mater. 168 (2013) 195–205.
[28] M. Boronat, A. Corma, What is measured when measuring acidity in zeolites with probe molecules, ACS Catal. 9 (2019) 1539–1548.
[29] A. Palčić, S.N. Jaén, D. Wu, M. Cai, C. Liu, E.A. Pidko, A.Y. Khodakov, V. Ordomsky, V. Valtchev, Embryonic zeolites for highly efficient synthesis of dimethyl ether from syngas, Microporous Mesoporous Mater. 322 (2021), 111138.
[30] M. Trombetta, G. Busca, M. Lenarda, L. Storaro, M. Pavan, An investigation of the surface acidity of mesoporous Al-containing MCM-41 and of the external surface of ferrierite through pivalonitrile adsorption, Appl. Catal. A: Gen. 182 (1999) 225–235.
[31] K. Góra-Marek, M. Derewiński, P. Sarv, J. Datka, IR and NMR studies of mesoporous alumina and related aluminosilicates, Catal. Today 101 (2005) 131–138.
[32] K. Gora-Marek, J. Datka, IR studies of OH groups in mesoporous alumino silicates, Appl. Catal. a-Gen. 302 (2006) 104–109.
[33] K. Tarach, K. Gora-Marek, J. Tekla, K. Brylewska, J. Datka, K. Mlekodaj, W. Makowski, M.C. Igualada Lopez, J. Martinez Triguero, F. Rey, Catalytic cracking performance of alkaline-treated zeolite Beta in the terms of acid sites properties and their accessibility, J. Catal. 312 (2014) 46–57.
[34] E. Rodríguez, R. Palos, A. Gutiérrez, F.J. Vela, J.M. Arandes, J. Bilbao, Effect of the FCC equilibrium catalyst properties and of the cracking temperature on the production of fuel from HDPE pyrolysis waxes, Energy Fuels 33 (2019) 5191–5199.
[35] J. Aguado, D.P. Serrano, J.M. Escola, A. Peral, Catalytic cracking of polyethylene over zeolite mordenite with enhanced textural properties, J. Anal. Appl. Pyrolysis 85 (2009) 352–358.
[36] K. Pyra, K.A. Tarach, E. Janiszewska, D. Majda, K. Góra-Marek, Evaluation of the textural parameters of zeolite beta in LDPE catalytic degradation: thermogravimetric analysis coupled with FTIR operando studies, Molecules 25 (2020) 926.
[37] K. Pyra, K.A. Tarach, K. Góra-Marek, Towards a greater olefin share in polypropylene cracking - amorphous mesoporous aluminosilicate competes with zeolites, Appl. Catal. B Environ. 297 (2021), 120408.
[38] A. Corma, V. González-Alfaro, A.V. Orchillés, The role of pore topology on the behaviour of FCC zeolite additives, Appl. Catal. A Gen. 187 (1999) 245–254.
[39] J. Abbot, Role of brønsted and lewis acid sites during cracking reactions of alkanes, Appl. Catal. 47 (1989) 33–44.
[40] G. Elordi, M. Olazar, G. Lopez, P. Castaño, J. Bilbao, Role of pore structure in the deactivation of zeolites (HZSM-5, Hβ and HY) by coke in the pyrolysis of polyethylene in a conical spouted bed reactor, Appl. Catal. B Environ. 102 (2011) 224–231.
[41] M.S. Renzini, L.C. Lerici, U. Sedran, L.B. Pierella, Stability of ZSM-11 and BETA zeolites during the catalytic cracking of low-density polyethylene, J. Anal. Appl. Pyrolysis 92 (2011) 450–455.
[42] E. Rodríguez, G. Elordi, J. Valecillos, S. Izaddoust, J. Bilbao, J.M. Arandes, P. Castaño, Coke deposition and product distribution in the co-cracking of waste polyolefin derived streams and vacuum gas oil under FCC unit conditions, Fuel Process. Technol. 192 (2019) 130–139.
[43] K.A. Tarach, K. Pyra, S. Siles, I. Melián-Cabrera, K. Góra-Marek, Operando study reveals the superior cracking activity and stability of hierarchical ZSM-5 catalyst for the cracking of low-density polyethylene, ChemSusChem 12 (2019) 633–638.
[44] I. Noda, Y. Ozaki, Principle of Two-Dimensional Correlation Spectroscopy, Two-Dimensional Correlation Spectroscopy – Applications in Vibrational and Optical Spectroscopy, John Wiley & Sons, Ltd,, 2005, pp. 15–38.
[45] C. Fernandez, I. Stan, J.-P. Gilson, K. Thomas, A. Vicente, A. Bonilla, J. Pérez-Ramírez, Hierarchical ZSM-5 zeolites in shape-selective xylene isomerization: role of mesoporosity and acid site speciation, Chem. A Eur. J. 16 (2010) 6224–6233.